

Contaminant Transport in Fractured Porous Media: Analytical Solution for a Single Fracture

D. H. TANG¹

Princeton University, Princeton, New Jersey 08540

E. O. FRIND AND E. A. SUDICKY

University of Waterloo, Waterloo, Ontario, Canada N2L 3G1

A general analytical solution is developed for the problem of contaminant transport along a discrete fracture in a porous rock matrix. The solution takes into account advective transport in the fracture, longitudinal mechanical dispersion in the fracture, molecular diffusion in the fracture fluid along the fracture axis, molecular diffusion from the fracture into the matrix, adsorption onto the face of the matrix, adsorption within the matrix, and radioactive decay. Certain assumptions are made which allow the problem to be formulated as two coupled, one-dimensional partial differential equations: one for the fracture and one for the porous matrix in a direction perpendicular to the fracture. The solution takes the form of an integral which is evaluated by Gaussian quadrature for each point in space and time. The general solution is compared to a simpler solution which assumes negligible longitudinal dispersion in the fracture. The comparison shows that in the lower ranges of groundwater velocities this assumption may lead to considerable error. Another comparison between the general solution and a numerical solution shows excellent agreement under conditions of large diffusive loss. Since these are also the conditions under which the formulation of the general solution in two orthogonal directions is most subject to question, the results are strongly supportive of the validity of the formulation.

INTRODUCTION

It is now widely recognized that fractures can play an important role in the transport of a contaminant in a groundwater system. Because the permeability of a fracture network is often substantially greater than the permeability of the host rock [see, e.g., *Wilson and Witherspoon*, 1970; *Nelson and Handin*, 1977; *Gale*, 1979], continuous fractures or fracture networks have the potential for being highly effective pathways for the transport of contaminants.

The problem of transport in fractured media arises, for example, in the case of a repository for radioactive waste built into a hard rock formation. Of prime concern here will be the critical path along which any radionuclides that may have escaped primary confinement can reach the biosphere. This critical path is likely to follow along fractures or fracture networks that are located near the repository or that form during its lifetime. Although the exact location of such fractures may be unknown, worst case predictions of travel time and of concentrations likely to occur at critical points can be instructive.

The problem also arises in the assessment of the protection that a fractured aquitard can provide to a freshwater aquifer against contamination from the ground surface or the atmosphere. An interesting example is discussed by *Day* [1977] and *Cherry et al.* [1979]. The prime question in this case is concerned with the level of contamination that can be expected at the bottom of an aquitard if a source of contamination is introduced at its top.

In the absence of losses a continuous open fracture would provide a virtually unobstructed travel path for a contaminant, and the protective effect of either a rock formation or a fractured aquitard would be low. Fortunately, an impor-

tant attenuation mechanism exists in the form of molecular diffusion into the solid matrix [*Golubev and Garibyants*, 1971]. This mechanism acts to reduce contaminant concentrations in the fracture and thereby delays the migration of the contaminant.

In the case of a radioactive contaminant the migration distance is finite because of decay. Diffusive loss into the matrix further reduces this finite migration distance. The porous matrix in this case may be viewed as a reservoir which holds the contaminant until decay occurs. Provided the source is constant, the distribution of the radionuclide in the system will reach an equilibrium state. The question of immediate interest is therefore: How far will the contaminant travel before it comes to equilibrium, and how long will it take?

A convenient way to study fracture-matrix transport is within the context of a single fracture. This problem is at present receiving considerable attention from researchers. One very recent paper is by *Neretnieks* [1980], who developed an analytical solution for transport in a fracture under the assumption that dispersion and diffusion along the fracture are negligible. Another recent work is by *Grisak and Pickens* [1980], who used the finite element technique to calculate concentrations in both the fracture and the matrix. An advantage of the numerical approach is that it admits any arbitrary boundary condition. A disadvantage is that the effects of numerical dispersion are difficult to assess.

It is the purpose of this paper (and its sequels) to develop general analytical solutions for the problem of contaminant transport in discrete fractures under consideration of all dispersive and diffusive processes. These solutions will be useful in the determination of penetration distances and response times. They will also be useful in evaluating the accuracy of special case solutions as well as numerical solutions.

THE PHYSICAL SYSTEM

We will consider the case of a thin rigid fracture situated in a saturated porous rock (Figure 1). The groundwater velocity

¹ Now at EXXON Production Research Company, Houston, Texas 77001.

in the fracture is assumed constant, and a contaminant source of constant strength exists at the origin of the fracture. We will make the following assumptions relating to the geometry and hydraulic properties of the system:

1. The width of the fracture is much smaller than its length.
2. Transverse diffusion and dispersion within the fracture assure complete mixing across the fracture width at all times.
3. The permeability of the porous matrix is very low and transport in the matrix will be mainly by molecular diffusion.
4. Transport along the fracture is much faster than transport within the matrix.

Assumptions 1 and 2 provide the basis for a one-dimensional representation of mass transport along the fracture itself. Assumptions 3 and 4 furthermore provide the basis for taking the direction of mass flux in the porous matrix to be perpendicular to the fracture axis. This results in the simplification of the basically two-dimensional system to two orthogonal, coupled one-dimensional systems. In this simplified form the problem is much more amenable to solution by analytical techniques.

The following processes are to be considered: (1) Advective transport along the fracture, (2) longitudinal mechanical dispersion in the fracture, (3) molecular diffusion within the fracture, in the direction of the fracture axis, (4) molecular diffusion from the fracture into the matrix, (5) adsorption onto the face of the matrix, (6) adsorption within the matrix, and (7) radioactive decay. Longitudinal mechanical dispersion describes the combined effects of mixing in the direction of the fracture axis due to the parabolic velocity profile [Taylor, 1953] and the roughness of the fracture walls. The processes of mechanical dispersion and molecular diffusion are usually lumped together as hydrodynamic dispersion [Bear, 1972]. Adsorption onto the fracture wall and adsorption within the porous matrix are considered separately here because of the possibility of differing chemical properties on the surface of the matrix. Adsorption processes are discussed in detail by Freeze and Cherry [1979].

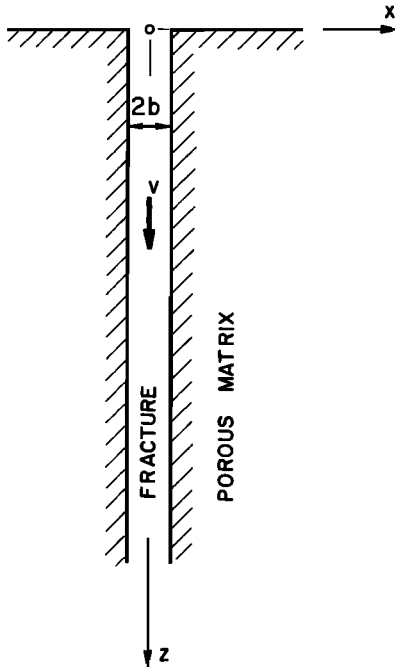


Fig. 1. Fracture-Matrix system.

GOVERNING EQUATIONS

The transport processes in the system of Figure 1 can be described by two coupled, one-dimensional equations, one for the fracture and one for the porous matrix. The coupling is provided by the continuity of fluxes and concentrations along the interface.

The differential equation for the fracture can be obtained by balancing the total mass of contaminant in the fracture. The equation is

$$v \frac{\partial c}{\partial z} - D \frac{\partial^2 c}{\partial z^2} + \frac{\partial c}{\partial t} + \frac{1}{b} \frac{\partial s}{\partial t} + \lambda c + \frac{\lambda}{b} s + \frac{q}{b} = 0 \quad 0 \leq z \leq \infty \quad (1)$$

where

- z coordinate along the fracture axis, L ;
- t time, T ;
- c concentration of solute in solution, equal to $c(z, t)$, M/L^3 ;
- s mass of solute adsorbed per unit length of fracture surface, equal to $s(z, t)$, M/L^2 ;
- $2b$ fracture width, L ;
- v groundwater velocity in the fracture, L/T ;
- λ decay constant, equal to $(\ln 2)/t_{1/2}$, $1/T$;
- $t_{1/2}$ half life, T ;
- q diffusive flux perpendicular to the fracture axis, M/L^2T .

The hydrodynamic dispersion coefficient D , (L^2/T) is further expressed as [Bear, 1972]

$$D = \alpha_L v + D^* \quad (2)$$

where α_L is the dispersivity in the direction of the fracture axis, (L), and D^* is the molecular diffusion coefficient in water (L^2/T).

We will assume that adsorption onto the fracture surface is governed by a linear equilibrium isotherm of the form $s = f(c)$. Accordingly, the dissolved and adsorbed phases are related by

$$s = \frac{ds}{dc} c = K_f c \quad (3a)$$

$$\frac{\partial s}{\partial t} = \frac{ds}{dc} \frac{\partial c}{\partial t} = K_f \frac{\partial c}{\partial t} \quad (3b)$$

where K_f is the distribution coefficient, defined by Freeze and Cherry [1979] as the mass of solute adsorbed per unit area of surface divided by the concentration of solute in solution. Upon substitution of (3) into (1) and introduction of the face retardation coefficient R , defined as

$$R = 1 + \frac{K_f}{b} \quad (4)$$

the differential equation for the fracture becomes

$$\frac{\partial c}{\partial t} + \frac{v}{R} \frac{\partial c}{\partial z} - \frac{D}{R} \frac{\partial^2 c}{\partial z^2} + \lambda c + \frac{q}{bR} = 0 \quad 0 \leq z \leq \infty \quad (5)$$

The diffusive loss term will be considered later.

The differential equation for the porous matrix can be obtained in a similar way by considering the mass balance for a strip of unit width, extending in the direction perpendicular to the fracture. This equation is

$$-D' \frac{\partial^2 c'}{\partial x^2} + \frac{\partial c'}{\partial t} + \frac{\rho_b}{\theta} \frac{\partial s'}{\partial t} + \lambda c' + \frac{\rho_b}{\theta} \lambda s' = 0 \quad b \leq x \leq \infty \quad (6)$$

where

- x coordinate perpendicular to the fracture axis, L ;
- c' concentration of solute in solution, equal to $c'(x, z, t)$, M/L^3 ;
- s' mass of solute adsorbed per unit mass of solid in the porous matrix, equal to $s'(x, z, t)$, M/M ;
- ρ_b bulk density of the matrix, M/L^3 ;
- θ porosity.

The effective diffusion coefficient D' is defined here as

$$D' = \tau D^* \quad (7)$$

where τ is the matrix tortuosity [Bear, 1972]. This form makes allowance for the fact that in a porous medium, molecular diffusion is constrained to follow certain tortuous paths within the pore structure. Alternative definitions of the effective diffusion coefficient may be found in the literature [see, e.g., Neretnieks, 1980].

For adsorption within the porous matrix we will assume a second linear equilibrium isotherm of the form $s' = g(c')$. Thus we obtain the relationships

$$s' = \frac{ds'}{dc'} c' = K_m c' \quad (8a)$$

$$\frac{\partial s'}{\partial t} = \frac{ds'}{dc'} \frac{\partial c'}{\partial t} = K_m \frac{\partial c'}{\partial t} \quad (8b)$$

where the distribution coefficient K_m is defined as [Freeze and Cherry, 1979] the mass of solute adsorbed per unit volume of solid divided by the concentration of solute in solution. Combining (6) and (8) and making use of the matrix retardation coefficient R' , defined as

$$R' = 1 + \frac{\rho_b}{\theta} K_m \quad (9)$$

yields the final differential equation for the matrix:

$$\frac{\partial c'}{\partial t} - \frac{D'}{R'} \frac{\partial^2 c'}{\partial x^2} + \lambda c' = 0 \quad b \leq x \leq \infty \quad (10)$$

We will now return to consideration of the diffusive loss term in (5). This term represents the diffusive mass flux crossing the fracture-matrix interface. This flux can be expressed by Fick's first law as

$$q = -\theta D' \left. \frac{\partial c'}{\partial x} \right|_{x=b} \quad (11)$$

The gradient $\partial c'/\partial x$ at the interface is obtainable by differentiation of the solution of (10). Equation (11) can be substituted into (5) to yield the final equation for the fracture, in coupled form

$$\frac{\partial c}{\partial t} + \frac{v}{R} \frac{\partial c}{\partial z} - \frac{D}{R} \frac{\partial^2 c}{\partial z^2} + \lambda c - \frac{\theta D'}{bR} \left. \frac{\partial c'}{\partial x} \right|_{x=b} = 0 \quad 0 \leq z \leq \infty \quad (12)$$

The boundary conditions for (12) are

$$c(0, t) = c_0 \quad (13a)$$

$$c(\infty, t) = 0 \quad (13b)$$

$$c(z, 0) = 0 \quad (13c)$$

where c_0 is the source concentration.

The boundary conditions for (10) are

$$c'(b, z, t) = c(z, t) \quad (14a)$$

$$c'(\infty, z, t) = 0 \quad (14b)$$

$$c'(x, z, 0) = 0 \quad (14c)$$

Equation (14a) expresses the coupling of the porous matrix to the fracture. The rationale for equating fracture and matrix concentrations at the interface is based on assumption 2 and the one-dimensional nature of (12). Its validity stands also in the presence of surface adsorption.

GENERAL TRANSIENT SOLUTION

We will first develop the general transient solution of the coupled system of equations (10), (12), (13), and (14). The solution strategy is, briefly, as follows: First, apply the Laplace transform to (10), solve the subsidiary equation, and express the concentration gradient at the interface in terms of its Laplace transform. Then apply the Laplace transform to (12), substitute for the interface gradient, and solve. Finally, invert the solution of (12), and the solution of (10).

Applying the Laplace transform to (10) yields

$$p\bar{c}' = \frac{D'}{R'} \frac{d^2 \bar{c}'}{dx^2} - \lambda \bar{c}' \quad (15)$$

where \bar{c}' is the Laplace transformation of c' , defined as

$$\bar{c}'(x, z, p) = \int_0^\infty \exp(-pt) c'(x, z, t) dt$$

The only physically admissible solution for (15) is of the form

$$\bar{c}' = c_1' \exp \{-BP^{1/2}(x - b)\} \quad (16)$$

where

$$B = (R'/D')^{1/2}$$

$$P = p + \lambda$$

The constant of integration c_1' in (16) is obtained by utilizing (14a). Equation (16) becomes

$$\bar{c}' = \bar{c} \exp \{-BP^{1/2}(x - b)\} \quad (17)$$

The gradient of \bar{c}' at the interface $x = b$ is

$$\left. \frac{d\bar{c}'}{dx} \right|_{x=b} = -BP^{1/2} \bar{c} \quad (18)$$

Proceeding to (12), we apply the Laplace transform and obtain

$$p\bar{c} + \frac{v}{R} \frac{d\bar{c}}{dz} + \lambda \bar{c} = \frac{\theta D'}{bR} \left. \frac{d\bar{c}'}{dx} \right|_{x=b} + \frac{D}{R} \frac{d^2 \bar{c}}{dz^2} \quad (19)$$

Upon substitution of (18), (19) becomes

$$\frac{d^2 \bar{c}}{dz^2} - \frac{v}{D} \frac{d\bar{c}}{dz} - \frac{R}{D} \left\{ P + \frac{P^{1/2}}{A} \right\} \bar{c} = 0 \quad (20)$$

where

$$A = \frac{bR}{\theta(R'D')^{1/2}}$$

Equation (20) is a second-order ordinary differential equation which has a solution of the form

$$\bar{c} = c_2 \exp(zr_+) + c_3 \exp(zr_-) \quad (21)$$

where c_2 and c_3 are undetermined constants and r takes on the two forms

$$r_{\pm} = \nu \left[1 \pm \left\{ 1 + \beta^2 \left(\frac{P^{1/2}}{A} + P \right) \right\}^{1/2} \right] \quad (22)$$

where

$$\nu = v/2D$$

$$\beta^2 = 4RD/v^2$$

Because the solution must be finite, the first term in (21) must vanish. We are thus left with

$$\bar{c} = c_3 \exp(\nu z) \exp \left[-\nu z \left\{ 1 + \beta^2 \left(\frac{P^{1/2}}{A} + P \right) \right\}^{1/2} \right] \quad (23)$$

The undetermined constant c_3 can be obtained by utilizing the boundary condition (13a). Applying the Laplace transform to this boundary condition yields

$$\bar{c}(0, p) = \frac{c_0}{p} = \frac{c_0}{p - \lambda} \quad (24)$$

which is seen to be the value of c_3 . Equation (23) thus becomes

$$\bar{c} = \frac{c_0}{p - \lambda} \exp(\nu z) \exp \left[-\nu z \left\{ 1 + \beta^2 \left(\frac{P^{1/2}}{A} + P \right) \right\}^{1/2} \right] \quad (25)$$

Equation (25) must now be inverted. A difficulty arises here from the fact that both P and $P^{1/2}$ appear inside the square root. This difficulty, however, can be overcome by making use of the identity

$$\int_0^\infty \exp \left(-\xi^2 - \frac{\chi^2}{\xi^2} \right) d\xi = \frac{\pi^{1/2}}{2} \exp(-2\chi) \quad (26)$$

We use this identity to convert the exponential term

$$\exp \left[-\nu z \left\{ 1 + \beta^2 \left(\frac{P^{1/2}}{A} + P \right) \right\}^{1/2} \right]$$

into the integral

$$\frac{2}{\pi^{1/2}} \int_0^\infty \exp \left[-\xi^2 - \frac{\nu^2 z^2}{4\xi^2} \left\{ 1 + \beta^2 \left(\frac{P^{1/2}}{A} + P \right) \right\} \right] d\xi$$

so that (25) appears as

$$\frac{\bar{c}}{c_0} = \frac{2}{\pi^{1/2}} \frac{1}{p - \lambda} \exp(\nu z) \int_0^\infty \exp(-\xi^2) \cdot \exp \left[-\frac{\nu^2 z^2}{4\xi^2} \left\{ 1 + \beta^2 \left(\frac{P^{1/2}}{A} + P \right) \right\} \right] d\xi \quad (27)$$

which can also be written as

$$\frac{\bar{c}}{c_0} = \frac{2}{\pi^{1/2}} \exp(\nu z) \int_0^\infty \exp \left[-\xi^2 - \frac{\nu^2 z^2}{4\xi^2} \right] \cdot \frac{\exp[-Y(P^{1/2} + AP)]}{p - \lambda} d\xi \quad (28)$$

where

$$Y = \frac{\nu^2 \beta^2 z^2}{4A\xi^2}$$

Thus the original variable c will be given in terms of the inverse transform L^{-1} as

$$\frac{c}{c_0} = \frac{2}{\pi^{1/2}} \exp(\nu z) \int_0^\infty \exp \left[-\xi^2 - \frac{\nu^2 z^2}{4\xi^2} \right] \cdot L^{-1} \left\{ \frac{\exp[-Y(P^{1/2} + AP)]}{p - \lambda} \right\} d\xi \quad (29)$$

To evaluate the inverse transform, we make use of the following two identities:

$$\begin{aligned} L^{-1} \left\{ \frac{\exp(-p^{1/2} Y)}{p - \gamma} \right\} \\ = \frac{1}{2} \exp(\gamma t) \left\{ \exp[-\gamma^{1/2} Y] \operatorname{erfc} \left[\frac{Y}{2t^{1/2}} - (\gamma t)^{1/2} \right] \right. \\ \left. + \exp[\gamma^{1/2} Y] \operatorname{erfc} \left[\frac{Y}{2t^{1/2}} + (\gamma t)^{1/2} \right] \right\} \end{aligned} \quad (30)$$

where erfc is the complementary error function, and

$$L^{-1} \{ \exp(-PE) \Phi(P) \} = \Phi(t - E) U(t - E) \quad (31)$$

where

$$\begin{aligned} U &= 0 & t < E \\ U &= 1 & t \geq E \end{aligned}$$

From (30) it follows that

$$\begin{aligned} L^{-1} \left\{ \frac{\exp(-YP^{1/2})}{p - \lambda} \right\} \\ = \frac{1}{2} \exp(\lambda t) \left\{ \exp[-\lambda^{1/2} Y] \operatorname{erfc} \left[\frac{Y}{2t^{1/2}} - (\lambda t)^{1/2} \right] \right. \\ \left. + \exp[\lambda^{1/2} Y] \operatorname{erfc} \left[\frac{Y}{2t^{1/2}} + (\lambda t)^{1/2} \right] \right\} \end{aligned} \quad (32)$$

Utilizing (31) and (32), we can express the inverse transform in (29) as

$$\begin{aligned} L^{-1} \left\{ \frac{\exp[-Y(P^{1/2} + AP)]}{p - \lambda} \right\} \\ = L^{-1} \left\{ \frac{\exp[-YP^{1/2}]}{p - \lambda} \exp(-YAP) \right\} \\ = \frac{1}{2} U(T^2) \exp(-\eta z^2) \left\{ \exp[-\lambda^{1/2} Y] \operatorname{erfc} \left[\frac{Y}{2T} - \lambda^{1/2} T \right] \right. \\ \left. + \exp[\lambda^{1/2} Y] \operatorname{erfc} \left[\frac{Y}{2T} + \lambda^{1/2} T \right] \right\} \end{aligned} \quad (33)$$

where

$$\begin{aligned} T &= \left(t - \frac{\nu^2 \beta^2 z^2}{4\xi^2} \right)^{1/2} = \left(t - \frac{Rz^2}{4D\xi^2} \right)^{1/2} \\ \eta &= \frac{\lambda R}{4D\xi^2} \end{aligned}$$

Substituting (33) into (29), we obtain

$$\frac{c}{c_0} = \frac{2}{\pi^{1/2}} \exp(\nu z) \int_0^\infty \exp \left[-\xi^2 - \frac{\nu^2 z^2}{4\xi^2} \right] \frac{1}{2} U(T^2) \exp(-\eta z^2) \cdot \left\{ \exp[-\lambda^{1/2} Y] \operatorname{erfc} \left[\frac{Y}{2T} - \lambda^{1/2} T \right] + \exp[\lambda^{1/2} Y] \operatorname{erfc} \left[\frac{Y}{2T} + \lambda^{1/2} T \right] \right\} d\xi \quad (34)$$

This equation can be simplified somewhat by making use of the fact that $T \geq 0$, which requires that

$$t \geq Rz^2/4D\xi^2$$

or

$$\xi \geq \frac{z}{2} \left(\frac{R}{Dt} \right)^{1/2}$$

Thus (34) becomes in final form

$$\frac{c}{c_0} = \frac{\exp(\nu z)}{\pi^{1/2}} \int_l^\infty \exp \left[-\xi^2 - \frac{\nu^2 z^2}{4\xi^2} \right] \exp(-\eta z^2) \cdot \left\{ \exp[-\lambda^{1/2} Y] \operatorname{erfc} \left[\frac{Y}{2T} - \lambda^{1/2} T \right] + \exp[\lambda^{1/2} Y] \operatorname{erfc} \left[\frac{Y}{2T} + \lambda^{1/2} T \right] \right\} d\xi \quad (35)$$

where

$$l = \frac{z}{2} \left(\frac{R}{Dt} \right)^{1/2}$$

is the lower limit of integration. Equation (35) is the solution for concentration in the fracture.

Finding the inverse transform for c' is now straightforward. From (17) we have

$$\frac{c'}{c_0} = \exp[-B(x-b)P^{1/2}] \frac{\bar{c}}{c_0} \quad (36)$$

and from (28) we have

$$\frac{\bar{c}}{c_0} = \frac{2}{\pi^{1/2}} \exp(\nu z) \int_0^\infty \exp \left[-\xi^2 - \frac{\nu^2 z^2}{4\xi^2} \right] \cdot L^{-1} \left\{ \frac{\exp[-(Y+B(x-b))P^{1/2} - YAP]}{P - \lambda} \right\} d\xi \quad (37)$$

Following the same procedure as was used in obtaining (35), (37) finally becomes

$$\frac{c'}{c_0} = \frac{\exp(\nu z)}{\pi^{1/2}} \int_l^\infty \exp \left[-\xi^2 - \frac{\nu^2 z^2}{4\xi^2} \right] \cdot \exp(-\eta z^2) \left\{ \exp[-\lambda^{1/2} Y'] \operatorname{erfc} \left[\frac{Y'}{2T} - \lambda^{1/2} T \right] + \exp[\lambda^{1/2} Y'] \operatorname{erfc} \left[\frac{Y'}{2T} + \lambda^{1/2} T \right] \right\} d\xi \quad (38)$$

where

$$Y' = \frac{\nu^2 \beta^2 z^2}{4A\xi^2} + B(x-b)$$

Equation (38) is the solution for concentration in the porous matrix.

TRANSIENT SOLUTION WITH $D = 0$

In order to demonstrate the effect of neglecting longitudinal dispersion in the fracture we will also present the solution for the special case with $D = 0$. Equation (12) is in this case reduced to a first-order equation. Inspection of (35) reveals that as $D \rightarrow 0$, the equation becomes singular; consequently, this special case cannot be expressed by the general solution.

Since (10) is unchanged, (15)–(18) hold also for the special case. Equation (19) now becomes

$$p\bar{c} + \frac{v}{R} \frac{d\bar{c}}{dz} + \lambda\bar{c} = \frac{\theta D'}{bR} \frac{d\bar{c}'}{dx} \bigg|_{x=b} \quad (39)$$

Upon substitution of (18), (39) becomes

$$\frac{v}{R} \frac{d\bar{c}}{dz} + \left\{ p + \lambda + \frac{P^{1/2}}{A} \right\} \bar{c} = 0 \quad (40)$$

The solution to (40) is of the form

$$\bar{c} = \frac{c_0}{p} \exp \left(-\frac{\lambda Rz}{v} \right) \exp \left(-\frac{pRz}{v} \right) \exp \left(-\frac{RP^{1/2}z}{vA} \right) \quad (41)$$

Using (30) and (31), the solution can be written as

$$\frac{c}{c_0} = 0 \quad T' < 0 \quad (42a)$$

$$\frac{c}{c_0} = \frac{1}{2} \exp \left(-\frac{\lambda Rz}{v} \right) \left[\exp \left(-\frac{\lambda^{1/2} Rz}{vA} \right) \operatorname{erfc} \left(\frac{z}{2vAT'} - \lambda^{1/2} T' \right) + \exp \left(\frac{\lambda^{1/2} Rz}{vA} \right) \operatorname{erfc} \left(\frac{z}{2vAT'} + \lambda^{1/2} T' \right) \right] \quad T' > 0 \quad (42b)$$

where

$$T' = \left(t - \frac{Rz}{v} \right)^{1/2}$$

Equations (42) express the concentration in the fracture.

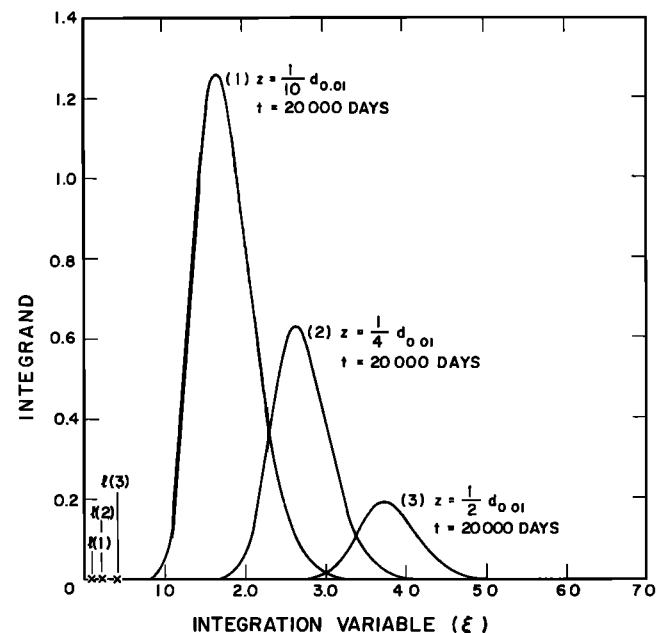


Fig. 2. Typical integrands for general solution, high-velocity case (the crosses indicate the lower limits of integration).

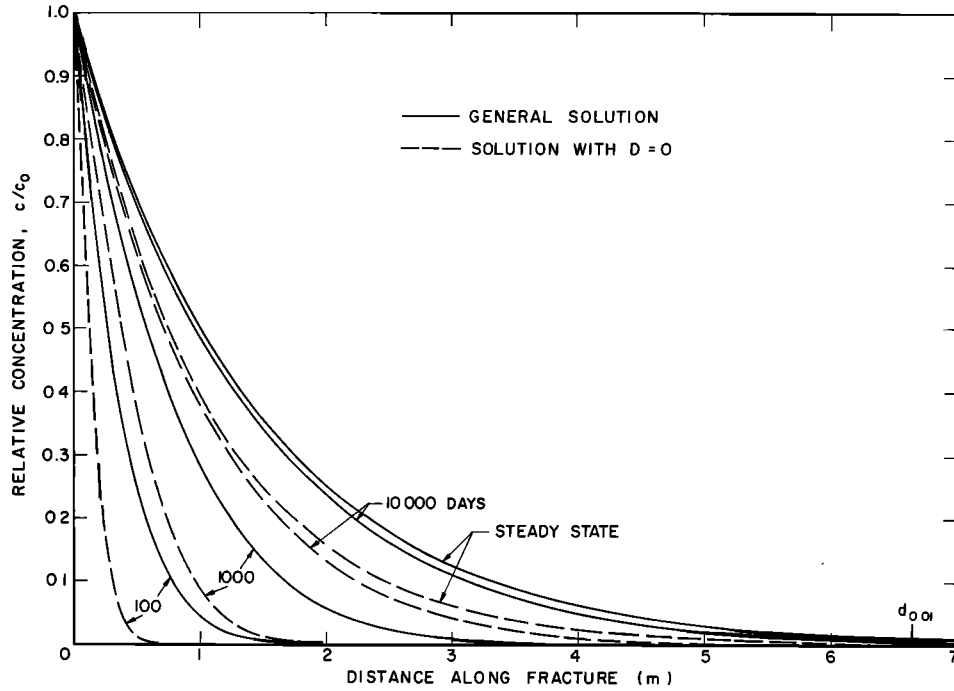


Fig. 3. Comparison with $D = 0$ solution, low-velocity case. Concentration profiles for the fracture at 100, 1000, and 10,000 days and at steady state.

To find the solution for the porous matrix, we combine (41) and (17) to obtain

$$c' = \frac{c_0}{p} \exp\left(-\frac{\lambda Rz}{v}\right) \exp\left(-\frac{pRz}{v}\right) \exp(-WP^{1/2}) \quad (43)$$

where

$$W = \frac{Rz}{vA} + B(x-b)$$

We invert (43) by making use of (30) and (31). This results in

$$\frac{c'}{c_0} = 0 \quad T' < 0 \quad (44a)$$

$$\begin{aligned} \frac{c'}{c_0} = \frac{1}{2} \exp\left(-\frac{\lambda Rz}{v}\right) & \left[\exp(-\lambda^{1/2}W) \operatorname{erfc}\left(\frac{W}{2T'} - \lambda^{1/2}T'\right) \right. \\ & \left. + \exp(\lambda^{1/2}W) \operatorname{erfc}\left(\frac{W}{2T'} + \lambda^{1/2}T'\right) \right] \quad T' > 0 \quad (44b) \end{aligned}$$

Equations (44) express the concentration in the porous matrix. It is obvious that (42) and (44) can be evaluated more easily than (35) and (38) because no integration is involved.

STEADY STATE SOLUTION

A steady state solution is most useful for the prediction of ultimate penetration distances. For steady state, (10) and (12) simplify to

$$D' \frac{d^2 c'}{dx^2} = \lambda c' \quad (45)$$

$$v \frac{dc}{dz} - D \frac{d^2 c}{dz^2} + \lambda c = \frac{\theta D'}{b} \frac{dc'}{dx} \bigg|_{x=b} \quad (46)$$

The solution of (45) is of the form

$$c' = c \exp\{-(\lambda/D')^{1/2}(x-b)\} \quad (47)$$

where we have made use of the interface boundary condition (14a). The concentration gradient at the interface is

$$\frac{dc'}{dx} \bigg|_{x=b} = -\left(\frac{\lambda}{D'}\right)^{1/2} c \quad (48)$$

Substitution of (48) into (46) yields

$$\frac{d^2 c}{dz^2} - \frac{v}{D} \frac{dc}{dz} - \frac{1}{D} \left\{ \lambda + \frac{(D'\lambda)^{1/2}}{b} \right\} c = 0 \quad (49)$$

The solution to (49) subject to the boundary conditions is

$$\frac{c}{c_0} = \exp\left\{\left[\nu - \left(\nu^2 + \frac{\psi}{D}\right)^{1/2}\right]z\right\} \quad (50)$$

where

$$\psi = \lambda + \frac{\theta(D'\lambda)^{1/2}}{b}$$

Substitution of (50) into (47) yields the solution for the porous matrix:

$$\frac{c'}{c_0} = \exp\left\{\left[\nu - \left(\nu^2 + \frac{\psi}{D}\right)^{1/2}\right]z\right\} \exp\left\{-\left(\frac{\lambda}{D'}\right)^{1/2}(x-b)\right\} \quad (51)$$

Note that the steady state solutions, both for the fracture and the matrix, are always of the exponential type, regardless of the values of v or D .

The steady state solution can be easily rearranged to express the steady state depth of penetration corresponding to some concentration level. For a concentration of $c/c_0 = \delta$, for example, the δ penetration depth into the fracture, d_δ , is obtained from (50) as

$$d_s = \frac{\ln \delta}{v - (v^2 + \psi/D)^{1/2}} \quad (52)$$

A similar expression can be obtained from (51) for the depth of penetration into the porous matrix.

EXAMPLES

We will first apply the general solution, the $D = 0$ solution, and the steady state solution to two cases selected to illustrate the effect of neglecting longitudinal dispersion in the fracture. Both cases have identical parameters except for the groundwater velocity in the fracture. The parameters are

$$\begin{aligned} 2b &= 100 \text{ } \mu\text{m} \\ \theta &= 0.01 \\ \tau &= 0.1 \\ \alpha_L &= 0.5 \text{ m} \\ D^* &= 1.6 \times 10^{-5} \text{ cm}^2/\text{s} \\ t_{1/2} &= 12.35 \text{ years} \\ R' &= 1.0 \\ R &= 1.0 \end{aligned}$$

The contaminant properties correspond to those of tritium [Foster, 1975]. The velocities in the fracture are

for the low-velocity case:

$$v = 0.01 \text{ m/d}$$

for the high-velocity case:

$$v = 0.1 \text{ m/d}$$

Inspection of (35) for the general transient solution shows that for each value of $c(z, t)$ the integral must be evaluated. The integration is most efficiently done by Gaussian quadrature. The integrand fortunately is generally well-behaved, taking on the form of a skewed bell-shaped curve. As an example, Figure 2 shows typical integrands for the high-velocity case, for points corresponding to $1/2$, $1/4$, and $1/10$ of $d_{0.01}$ at a time of 20,000 days. The curves obtained for most choices of parameters are similar to those shown here.

Although the integrand theoretically extends from l to infinity, the numerically significant portion generally extends over a much smaller range. It is evident in Figure 2 that the lower limit of integration is below the point where the in-

tegrand becomes numerically significant. Because of this, each curve is first scanned prior to integration to determine its range; then the integration points are located within the range. In using this scheme, from 20 to 60 Gauss points are usually found to give an integration that is virtually exact. Approximately 1 s of execution time is required on an IBM 3031 to calculate the concentration in the fracture at a single point when 60 Gauss points are used. The evaluation of (38) is performed in a similar way.

The results for the low-velocity case are plotted in Figures 3–5. Figure 3 shows concentration profiles along the fracture at 100, 1000, and 10,000 days as well as at steady state. The 1% penetration depth ($d_{0.01}$) is 6.66 m. It is evident that the $D = 0$ solution lags substantially behind the general solution at all times. In terms of steady state penetration depth the lag amounts to about 25% of the concentration obtained with the general solution. The magnitude of this lag would appear to indicate that at low groundwater velocities the effect of longitudinal dispersion in the fracture should not be ignored. Figure 4 shows the steady state concentration profiles for the porous matrix at three points corresponding to $1/2$, $1/4$, and $1/10$ of the 1% penetration depth $d_{0.01}$. It is seen that the lag between the general solution and the $D = 0$ solution extends for some distance into the porous matrix. Figure 5 shows the breakthrough curves for the fracture concentrations in the low-velocity case for the same points. It is seen that the concentrations reach at least 90% of their final values within about 10,000 days. Full equilibrium is essentially attained at about 20,000 days.

The next three figures are concerned with the high-velocity case. Figure 6 shows concentration profiles along the fracture, again at 100, 1000, and 10,000 days and at equilibrium. The 1% penetration depth $d_{0.01}$ in this case is increased to 51.3 m. Although the velocity is the only parameter that was changed, the increase in penetration depth is obviously not proportional to the velocity increase because it is also affected by the diffusive loss and the longitudinal dispersion. Except for the scale change the shape of the concentration profiles for the general solution is essentially the same as that for the low-velocity case. The lag between the general solution and the $D = 0$ solution, however, is now reduced to about 5%. Figure 7 shows the steady state concentration profiles for the porous

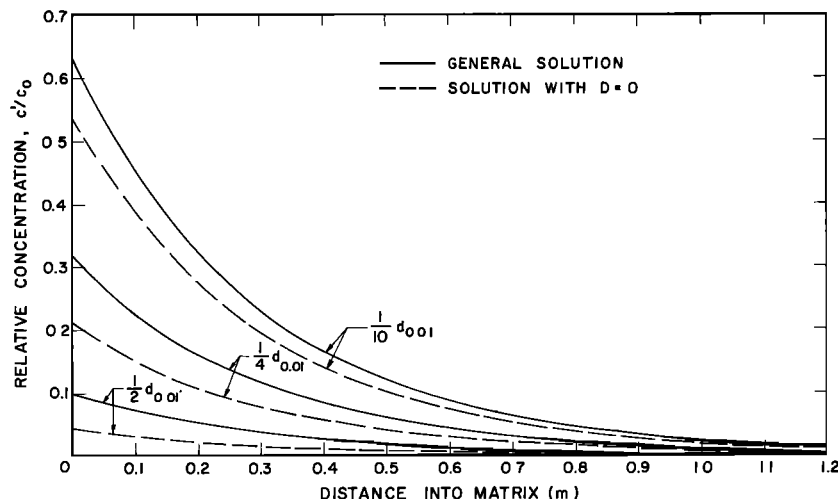


Fig. 4. Comparison with $D = 0$ solution, low-velocity case. Steady state concentration profiles for the porous matrix at $z = 1/2, 1/4$, and $1/10 d_{0.01}$.

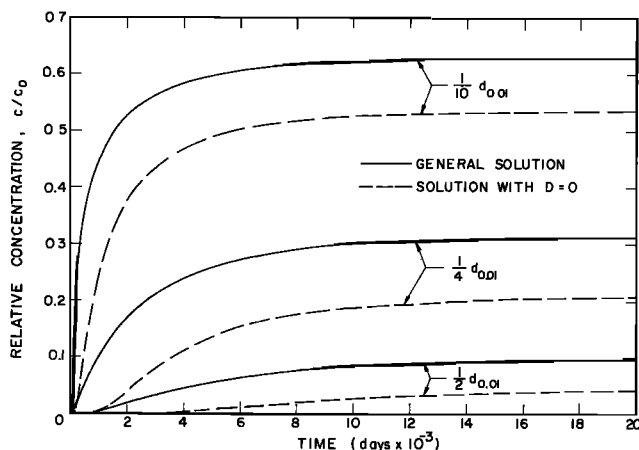


Fig. 5. Comparison with $D = 0$ solution, low-velocity case. Breakthrough curves for the fracture at $z = 1/2$, $1/4$, and $1/10 d_{0,01}$.

matrix, again at $1/2$, $1/4$, and $1/10$ of $d_{0,01}$. The penetration depth into the matrix is seen to be the same as for the low-velocity case. Figure 8 shows the breakthrough curves for the fracture concentrations in the high-velocity case. These are very similar to those in the low-velocity case except for a slightly less rapid rise at early time. In comparing the breakthrough curves for the two cases it must be kept in mind that they correspond to points whose location is not the same for the two cases. Equilibrium is reached at about the same time, however, in both cases.

In Figures 9 and 10 the results of the general solution are compared to fracture concentrations obtained by *Grisak and Pickens* [1980], who used the finite element method. The following parameters are used here:

$$\begin{aligned} 2b &= 120 \mu\text{m} \\ \theta &= 0.35 \\ \alpha_L &= 0.76 \text{ m} \\ v &= 0.75 \text{ m/d} \end{aligned}$$

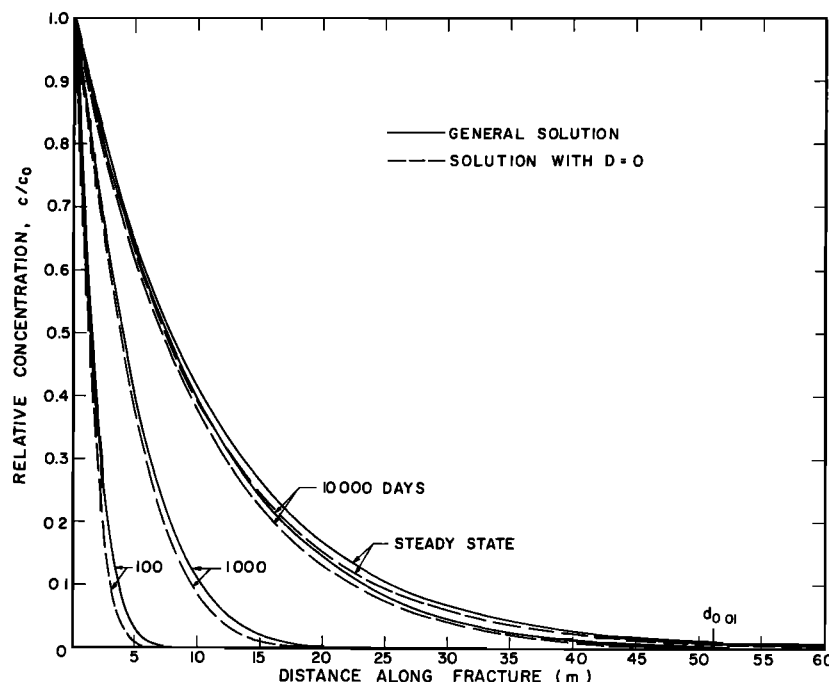


Fig. 6. Comparison with $D = 0$ solution, high-velocity case. Concentration profiles for the fracture at 100, 1000, and 10,000 days and at steady state.

The effective diffusion coefficient for the porous matrix, D' , is varied in the range from 0.0 to $10^{-6} \text{ cm}^2/\text{s}$, which is representative of most geologic media. Decay and retardation are not considered.

It should be noted that the system used in the numerical simulation differs somewhat from that used in the analytical solution because the input zone includes the upper surface of the matrix ($z = 0$), an approximation to a parabolic velocity profile is specified in the fracture, and the porous matrix is intersected by multiple parallel fractures such that $\partial c/\partial x = 0$ along the centerline of a matrix block. However, no response was obtained at the matrix block centerline during the first 4 days of the numerical simulation except in the upper portion of the matrix near the source.

It can be seen from Figures 9 and 10 that excellent agreement between the two solutions is obtained for values of $D' = 10^{-6} \text{ cm}^2/\text{s}$ at all times and $D' = 10^{-7} \text{ cm}^2/\text{s}$ for times greater than 3 days. These values are representative of relatively high rates of matrix diffusion and, consequently, relatively large penetration distances into the matrix and relatively small penetration distances down the fracture. With increasing matrix diffusion the concentration gradient in the matrix would tend to deviate more from the perpendicular direction we have assumed in the formulation of the general solution. The agreement with the two-dimensional numerical solution suggests that the assumption of orthogonality for the analytical solution is reasonable. It also appears that distributing the source along the upper surface of the matrix has little effect in this case because transport in the fracture is much more rapid than transport in the matrix. Similarly, there seems to be no significant advantage to including a parabolic velocity profile in the fracture instead of the average velocity. The good agreement can be seen as a verification of the analytical solution under conditions where its formulation in terms of two coupled, one-dimensional equations is most likely to be questioned.

A much poorer agreement exists between the general tran-

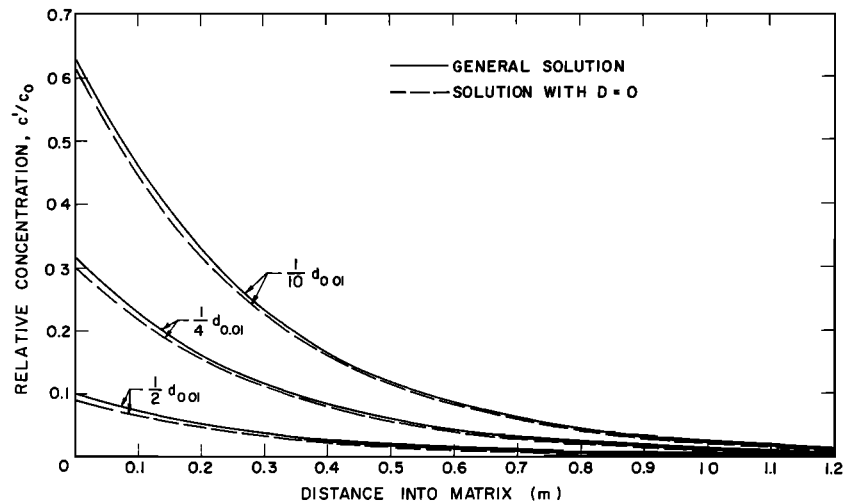


Fig. 7. Comparison with $D = 0$ solution, high-velocity case. Steady state concentration profiles for the porous matrix at $z = 1/2, 1/4$, and $1/10 d_{0.01}$.

sient solution and the numerical solution in the middle range of values of D' between 10^{-8} and 10^{-9} cm²/s and for $D' = 10^{-7}$ cm²/s at early time. The discrepancy appears in both the profiles of Figure 9 and the breakthrough curves of Figure 10. Since the general analytical solution can be considered to be accurate in this range on the basis of the above findings, the discrepancies are likely the result of insufficient discretization in the numerical solution near the fracture interface. For values of diffusion coefficients in this range, large gradients develop at the interface, and unless a very fine discretization is used, considerable error can be introduced in the numerical estimation of the diffusive flux.

Excellent agreement is again obtained for $D' = 10^{-10}$ cm²/s and for the case of no diffusive loss. The latter case was obtained from the general solution by letting the matrix porosity equal zero. As the diffusion coefficient approaches zero, the importance of the diffusive loss decreases, and the discretization error embedded in the loss term in the numerical solution thus has a less profound effect on the transport of solutes in the fracture. In general, the numerical solution is seen to be most susceptible to discretization error in the middle range of values of the diffusion coefficient, while at both the

upper end and the lower end of the range it is much less susceptible.

CONCLUSION

The general analytical solution is based on a number of assumptions whose validity depends on the configuration of the particular system. Conditions under which these assumptions may be questioned are those where the diffusive loss into the porous matrix is large, as such conditions tend to produce relatively short penetration distances down the fracture and relatively large penetration distances into the matrix. This would tend to result in (1) a generally two-dimensional mass distribution in the porous matrix, (2) a relatively greater importance of the variation in concentration across the thickness of the fracture, and (3) a relatively greater importance of mass influx at the top surface of the matrix. These factors are neglected in the analytical solution. The same conditions, however, tend to be favorable to the numerical solution [Grisak and Pickens, 1980], which takes all of these factors into account explicitly and which is least susceptible to discretization error when transport down the fracture and transport into the

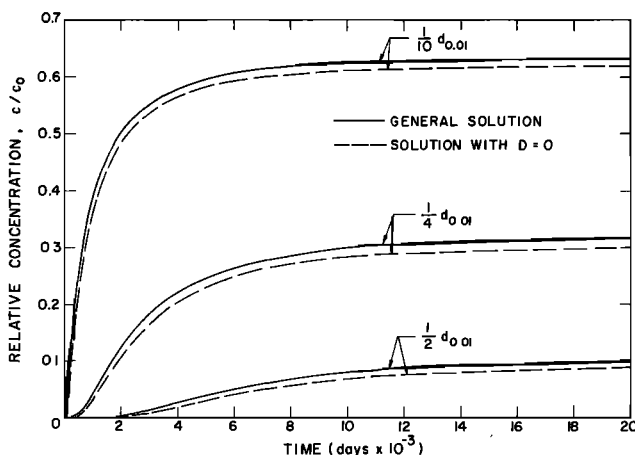


Fig. 8. Comparison with $D = 0$ solution, high-velocity case. Breakthrough curves for the fracture at $z = 1/2, 1/4$, and $1/10 d_{0.01}$.

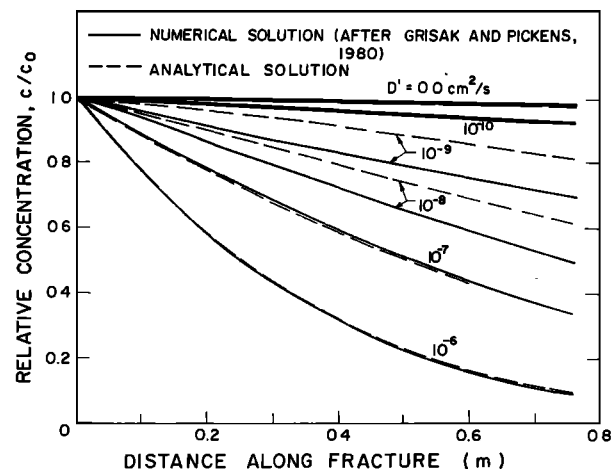


Fig. 9. Comparison with numerical solution of Grisak and Pickens [1980]. Concentration profiles for the fracture at 4 days, for values of D' in the range of 10^{-6} to 10^{-10} cm²/s and for no diffusion.

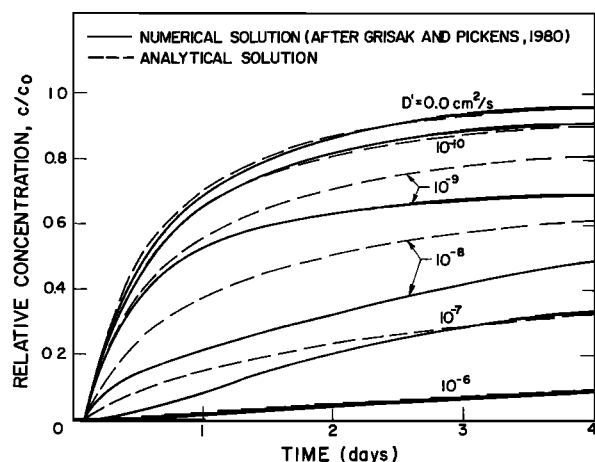


Fig. 10. Comparison with numerical solution of *Grisak and Pickens* [1980]. Breakthrough curves for fracture at $x = 0.76$ m, for values of D' in the range of 10^{-6} to 10^{-10} cm^2/s and for no diffusion.

matrix are nearly equal. The excellent agreement between the two solutions in the case of large diffusive loss can be taken as being strongly supportive of the validity of the assumptions underlying the general analytical solution.

Comparison of the general solution with the solution for the special case of negligible longitudinal dispersion shows that for relatively low velocities the effect of longitudinal dispersion in the fracture may be significant.

The analytical solution allows the determination of the ultimate penetration of a contaminant along a single fracture and the time taken to reach this penetration. Although the system assumed is highly idealized, the solution provides valuable insight into the mechanics of transport in fracture-matrix systems.

The results show that matrix diffusion can be viewed as a valuable safety mechanism in potential contamination problems involving a concentrated source in fractured rock. This safety mechanism will depend strongly on the transport parameters; for example, in a system with large matrix porosity and low fracture fluid velocity it will be much more effective than in a system with low matrix porosity and high fracture fluid velocity.

In subsequent papers we will investigate this safety mechanism in more detail. We will also consider systems of parallel fractures.

Acknowledgments. The authors benefitted greatly, throughout the course of the study, by discussions with John Cherry and Peter Fritz of the University of Waterloo on the practical aspects of contaminant transport in groundwater. In the final stages, Ken Dormuth of Atomic Energy of Canada Ltd. provided valuable input on theoretical aspects. The assistance of Bill Blackport in the creation of the computer codes is highly appreciated. Financial support for this study was provided through a research contract by Atomic Energy of Canada Limited, Whiteshell Nuclear Research Establishment, Pinawa, Manitoba.

REFERENCES

- Bear, J., *Dynamics of Fluids in Porous Media*, Elsevier, New York, 1972.
- Cherry, J. A., D. E. Desaulniers, E. O. Frind, P. Fritz, D. M. Gevaert, R. W. Gillham, and B. LeLievre, Hydrogeologic properties and pore-water origin and age: Clayey till and clay in south-central Canada, paper presented at the Workshop in Low-Flow Low-Permeability Measurements in Largely Impermeable rocks, OECD Nucl. Energ. Agency and Int. At. Energ. Agency, Paris, March 1979.
- Day, M. J., Analysis of movement and hydrochemistry of groundwater in the fractured clay and till deposits of the Winnipeg area, Manitoba, M.Sc. thesis, Univ. of Waterloo, Waterloo, Ont., 1977.
- Foster, S. S. D., The Chalk groundwater tritium anomaly—A possible explanation, *J. Hydrol. Amsterdam*, 25, 159–165, 1975.
- Freeze, R. A., and J. A. Cherry, *Groundwater*, Prentice-Hall, Englewood Cliffs, N. J., 1979.
- Gale, J. E., Assessing the permeability characteristics of fractured rock, paper presented at the Conference on Recent Trends in Hydrogeology, Lawrence Berkeley Lab., Berkeley, Calif., 1979.
- Golubev, V. S., and A. A. Garibyants, *Heterogeneous Processes of Geochemical Migration*, translated from Russian by J. P. Fitzsimmons, Consultants Bureau, New York, 1971.
- Grisak, G. E., and J. F. Pickens, Solute transport through fractured media, 1, The effect of matrix diffusion, *Water Resour. Res.*, 16(4), 719–730, 1980.
- Nelson, R. A., and J. Handin, Experimental study of fracture permeability in porous rock, *Am. Assoc. Pet. Geol. Bull.*, 61(2), 227–236, 1977.
- Neretnieks, I., Diffusion in the rock matrix: An important factor in radionuclide retardation? *J. Geophys. Res.*, 85(B8) 4379–4397, 1980.
- Taylor, G. E., Dispersion of soluble matter in solvent flowing slowly through a tube, *Proc. R. Soc. London, Ser. A*, 1137(219), 186–203, 1953.
- Wilson, C. R., and P. A. Witherspoon, An investigation of laminar flow in fractured porous rocks, *Publ. 70-6*, Dep. of Civ. Eng., Univ. of Calif., Berkeley, 1970.

(Received April 22, 1980;
revised October 31, 1980;
accepted November 12, 1980.)